RSC Advances

PAPER

View Article Online
View Journal | View Issue

Cite this: *RSC Adv.*, 2025, **15**, 1220

Drimane-type sesquiterpenoids and triterpenoids from the whole plant of *Limonium sinense* with their antiproliferative and anti-inflammatory activities†

Shizhou Qi, *[ab] Xinyu Meng,[a] Bingjie Cui,[b] Tingting Liu,[b] Lijuan Yang,[b] Guowei Cai,[c] Kaikai Gong *[b] and Shuang Miao*[b]

Received 18th September 2024
Accepted 21st November 2024

DOI: 10.1039/d4ra06721e

rsc.li/rsc-advances

Saline-tolerant medicinal plants possess novel chemical constituents with high bioactivity because of their unique secondary metabolic pathways. *Limonium sinense,* an aquatic plant found in the coastal wetlands of the Yellow River Delta, was collected and studied in the present work. Ten drimane-type sesquiterpenoids and four triterpenoids, including six new ones (sinenseines A–F), were isolated from a whole plant of *L. sinense* for the first time. Their structures, including the absolute configurations, were determined by analyzing the comprehensive spectroscopic data. In addition, twelve terpenoids, including nine sesquiterpenoids, were identified using UPLC-MS/MS and GNPS methods. All isolates were evaluated for their antiproliferative and anti-inflammatory activities. Compounds **2–4**, **6**, **13**, and **14** showed moderate anti-tumor effects on A549, H1299, HepG2 and A2780 cells with IC_{50} values ranging from 35.2 ± 2.0 to 90.5 ± 3.1 μM. Furthermore, compound **1** exhibited significant anti-inflammatory activity with an IC_{50} value of 8.3 ± 1.2 μM against NO production in LPS-induced RAW 264.7 macrophages.

Introduction

The identification of natural products with new structures and high bioactivity from medicinal plants has always been considered an important approach to drug development. The Yellow River Delta (YRD), the broadest coastal wetland of the warm tropics in Binzhou and Dongying city of China, is rich in saline-tolerant medicinal plants.[1] Reported data reveal that more than 262 kinds of medicinal plants are found in YRD.[2] In particular, *Apocynum venetum*, *Scorzonera mongolica*,*Subergorgia reticulata* and some other plants are considered the characteristic plants of YRD. These plants might possess potential lead compounds because of the unique high salinity and high alkaline environment prevalent in the YRD. Although YRD has abundant medicinal plant resources, there are very few studies on the chemical constituents and bioactivity of these plants. In order to explore the application value of the medicinal plants in this region and to enrich their phytochemical and pharmacological properties, *L. sinense* was selected, collected and studied in this work.

Limonium sinense (Girard) Kuntze (Plumbaginaceae) is a well-known medicinal plant and landscape plant, which is mainly distributed in the seashores and salt marshes of China.[3] In China, *L. sinense* is called "Shi-Ye-Cao" or "Hai-Jin-Hua", and the whole plant of *L. sinense* is used to treat fever, hemorrhage and menstrual disorders.[4] Recent studies revealed that *L. sinense* extracts possess anti-tumor, anti-viral, hepatoprotective and immunomodulatory activities.[5–8] In addition, *L. sinense* is an excellent sand-fixation plant because of its strong tolerance to drought stress and salt stress.[2] Until now, only a few phytochemical investigations on *L. sinense* have been reported, describing the presence of bioactive compounds, such as flavonoids and phenolics, with anti-tumor, anti-viral and immunomodulatory activities.[9] In this work, we isolated ten drimane-type sesquiterpenoids, including six molecules named sinenseines A–F and four known analogues, as well as four triterpenoids, from the whole plant of *L. sinense* for the first time. Their isolation process, structure determination, and anti-proliferative and anti-inflammatory activity evaluation are also described. Furthermore, ultra-performance liquid chromatography coupled with tandem mass spectrometry (UPLC-MS/MS), global natural product social molecular networking (GNPS) and database comparison methods were used to identify more terpenoids present in *L. sinense*.

[a]*Department of Pharmacy, Binzhou Medical University Hospital, Binzhou 256603, China. E-mail: qishizhou@126.com*

[b]*Medical Research Center, Binzhou Medical University Hospital, Binzhou 256603, China. E-mail: gongkaikai1005@163.com; keaimiaoshuang@126.com*

[c]*National Drug Clinical Experimental Organization, Binzhou Medical University Hospital, Binzhou 256603, China*

† Electronic supplementary information (ESI) available. See DOI: https://doi.org/10.1039/d4ra06721e

Results and discussion

Structural elucidation

Compound **1** was obtained as an amorphous light-yellow solid. The molecular formula was assigned as $C_{15}H_{20}O_3$ according to the HRESIMS data (*m/z* 247.1340 $[M - H]^-$, calcd 247.1334), indicating six degrees of unsaturation. The ^{1}H NMR spectrum of **1** (Table 1) revealed the presence of an oxygenated methylene at δ_H 4.76 (2H, dd, J = 17.4, 7.8 Hz) and three single methyl groups at δ_H 1.09 (3H, s), 1.08 (3H, s) and 1.00 (3H, s). The ^{13}C NMR spectrum of **1** (Table 2), as well as its ^{1}H NMR and HSQC spectra, disclosed 15 resonances, including a ketone carbonyl carbon at δ_C 215.6, an ester carbonyl carbon at δ_C 171.9, two olefinic carbons at δ_C 161.5 and 131.9, five methylene carbons at δ_C 70.7, 33.5, 32.3, 24.4, and 18.9, a methine carbon at δ_C 50.5, two quaternary carbons at δ_C 46.4 and 33.4, and three methyl groups at δ_C 26.7, 20.5 and 19.0. The ^{1}H and ^{13}C NMR spectra of **1** indicated that the structure of **1** was a bicyclic sesquiterpenoid, and the drimane-type sesquiterpenoid skeleton of **1** was deduced by comparing with data of **9** (7-ketoisodrimenin), an analogue with the same molecular weight.[10] The only difference between **1** and **9** was the position of the ketone carbonyl group. Although all HMBC correlations of the ketone carbonyl carbon in **1** with ^{1}H NMR signals were not recorded because of the program of the Bruker spectrometer, the position of the ketone carbonyl group of **1** could be easily deduced by the key HMBC correlations of δ_H 2.46/2.31 (H-7) with δ_C 50.1 (C-5), 18.9 (C-6), 161.5 (C-8) and 131.9 (C-9) (Fig. 2). In addition, a very clear difference in the chemical shift of the carbonyl group at C-3 ($\delta_C \approx 215$) and C-7 ($\delta_C \approx 196$) also supported this deduction. The total NMR data of **1** were obtained by a combined analysis of the 1D and 2D NMR data, including ^{1}H NMR, ^{13}C NMR, HSQC and HMBC. From the biogenetic point of view, the relative configurations at C-5 and C-10 in **1** were the same as those in drimenin; CH_3-15 was β-oriented, and H-5 was α-oriented. In addition, a NOESY spectrum (Fig. 3) was obtained to establish the relative configuration of **1**, in which the cross-peaks of CH_3-13/CH_3-15 and CH_3-14/H-5 indicated that CH_3-13/15 was β-oriented, and CH_3-14/H-5 was α-oriented. To define the absolute configuration, electronic circular dichroism (ECD) calculation was performed at the B3LYP/6-31G(d,p) level according to a time-dependent density functional theory (TD-DFT) method using the Gaussian 09 program. Finally, the agreement of the Cotton effects of the calculated and experimental ECD spectra allowed the assignment of the absolute configuration of **1** to 5*R*, 10*S* (Fig. 4). Therefore, compound **1** was established as 3-ketoisodrimenin and named sinenseine A.

Table 2 ^{13}C NMR spectral data of compounds **1–6** (150 MHz, DMSO-d_6)

No.	1	2	3	4	5	6
1	32.3	37.8	38.1	32.5	31.4	40.2
2	33.5	34.1	34.7	25.5	26.6	18.1
3	215.6	214.6	215.8	74.1	75.8	35.7
4	46.4	46.8	47.3	37.3	38.3	37.6
5	50.1	49.4	51.2	42.9	50.0	42.3
6	18.9	23.4	23.9	23.3	35.6	23.3
7	24.4	123.0	122.3	124.0	195.9	123.9
8	161.5	129.8	134.7	130.0	149.8	129.8
9	131.9	60.4	55.8	61.7	149.7	60.0
10	33.4	34.8	35.7	35.5	35.7	35.5
11	70.7	173.1	59.4	173.5	67.4	174.0
12	171.9	21.1	22.2	21.7	171.0	21.7
13	26.7	25.1	22.3	28.9	27.5	70.2
14	20.5	21.8	14.3	22.6	15.3	18.3
15	19.0	14.4	25.6	15.1	17.6	15.8
OCH_3			50.6			

Table 1 ^{1}H NMR spectral data of compounds **1–6** (600 MHz, DMSO-d_6)

No.	1	2	3	4	5	6
1	2.53, m	1.96, m	2.27, m	1.79, m	2.42, m	1.64, d (12.6)
	1.66, m	1.67, m	1.50, m	1.27, m	1.39, m	1.17, m
2	2.53, m	2.74, td (14.4, 5.4)	2.73, td (14.4, 5.4)	1.79, m	1.62, m	1.50, m
		2.14, dt (14.4, 5.4)	2.11, dt (14.4, 4.2)	1.44, m		1.44, m
3				3.24, m	3.10, dd (13.2, 6.6)	1.44, m
						1.17, m
5	1.80, m	1.58, dd (12.6, 4.2)	1.51, dd (12.6, 4.2)	1.55, m	1.84, m	1.50, m
6	1.80, m	2.05, m	2.00, m	1.86, m	2.67, m	1.92, m
	1.56, m	1.96, m	1.86, m		2.42, m	1.81, m
7	2.46, m	5.53, t (1.8)	5.44, m	5.48, t (1.8)		5.46, s
	2.31, m					
9		2.83, s	1.80, brs	2.77, s		2.74, s
11	4.72, m		3.65, dd (10.8, 5.4)		4.88, s	
			3.52, dd (10.8, 5.4)			
12		1.61, s	1.71, s	1.57, s		1.57, s
13	1.08, s	0.97, s	1.02, s	0.89, s	0.93, s	3.15, d (10.8)
						2.85, d (10.8)
14	1.00, s	1.03, s	0.97, s	0.85, s	0.80, s	0.75, s
15	1.09, s	1.08, s	0.95, s	0.84, s	1.19, s	0.91, s
OCH_3			3.17, s			
OH				4.27, d (4.8)	4.60, d (4.8)	4.52, s
COOH		12.29, s		12.06, s		12.00, brs

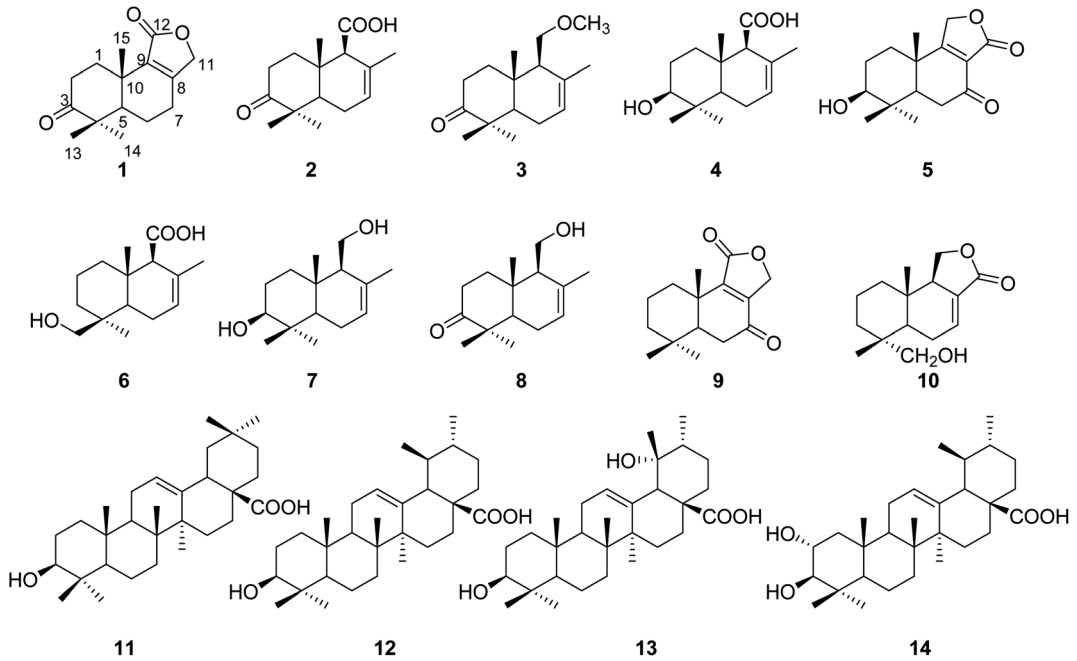

Fig. 1 Structures of compounds **1–14**.

Compound **2** was obtained as an amorphous yellow solid. Its molecular formula $C_{15}H_{22}O_3$ was determined on the basis of the HRESIMS signal at *m*/*z* 249.1496 $[M - H]^-$ (calcd for $C_{15}H_{21}O_3$, 249.1491), revealing five degrees of unsaturation. The ^{1}H NMR spectrum of **2** (Table 1) showed four single methyl groups at δ_H 1.61 (3H, s), 1.08 (3H, s), 1.03 (3H, s) and 0.97 (3H, s), an olefinic proton at δ_H 5.53 (1H, t, $J = 1.8$ Hz), and a carboxyl proton at δ_H 12.29 (1H, s). The ^{13}C NMR spectrum of **2** together with its HSQC spectrum revealed 15 resonances, including a ketone carbonyl carbon at δ_C 214.6, a carboxyl carbon at δ_C 173.1, two olefinic carbons at δ_C 129.8 and 123.0, and four methyl carbons at δ_C 25.1, 21.8, 21.1 and 14.8. The ^{1}H and ^{13}C NMR data of **2** were very similar to those of **8**, with the only difference being the replacement of a hydroxymethyl group [δ_H 3.82 (1H, d, $J = 10.8$, 5.4 Hz), 3.87 (1H, d, $J = 10.8$, 5.4 Hz), δ_C 60.4] by a carboxyl group [δ_H 12.29 (1H, s), δ_C 173.1]. The planar structure of **2** was established based on the above 1D and 2D NMR data. The α-orientation of H-9 was deduced from the ROESY cross-peak between H-9 and H-5. The ROESY correlations of CH_3-13/CH_3-15 in **2** indicated that CH_3-13/15 were β-oriented (Fig. 3). The absolute configuration of (5*R*,9*S*,10*S*)-**2** was defined based on the good agreement between the calculated and the experimental ECD curves (Fig. 4). Therefore, compound **2** was established as 3-ketodrimenoic acid and named sinenseine B.

Compound **3**, an amorphous light yellow solid, possessed the molecular formula $C_{16}H_{26}O_2$ according to the HRESIMS signal at *m*/*z* 249.1485 $[M - H]^-$ (calcd for $C_{16}H_{25}O_2$, 249.1491), with four degrees of unsaturation. Its ^{1}H NMR and HSQC spectra disclosed 15 resonances, including a ketone carbonyl unsaturation. The ^{1}H and ^{13}C NMR spectra (Table 1) of **3** exhibited similarities with those of **8**, suggesting the presence of the same drimane-type sesquiterpenoid skeleton. The only difference between their NMR signals was the replacement of the hydroxyl group by a methoxyl group in **3**. The relative stereochemistry was established by ROESY experiments, and the correlations from CH_3-14 to H-9 and H-5 to H-9 suggested that CH_3-14, H-5 and H-9 were α-oriented. The β orientation of CH_3-13/15 was assigned based on the correlation of CH_3-13/15 (Fig. 3). By comparing the calculated ECD curve with the experimental curve, the absolute configuration of **3** was elucidated as 5*R*,9*S*,10*S* (Fig. 4). Therefore, the structure of compound **3** was assigned as shown in the figure and named sinenseine C.

Compound **4** was purified as an amorphous yellow solid and assigned the molecular formula $C_{15}H_{24}O_3$ according to the HRESIMS data (*m*/*z* 251.1652 $[M - H]^-$, calcd 251.1647). The ^{1}H and ^{13}C NMR data (Table 1) of **4** suggested its close similarity to compound **2**, except that the ketone carbonyl group was

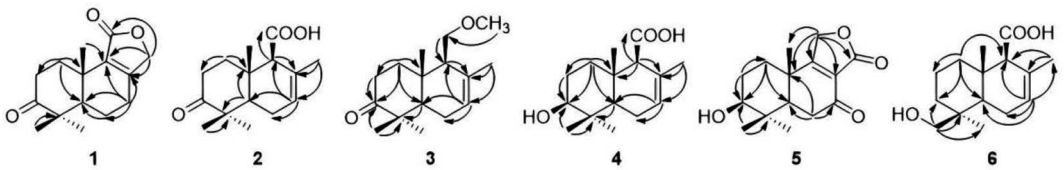

Fig. 2 Key HMBC correlations of compounds **1–6**.

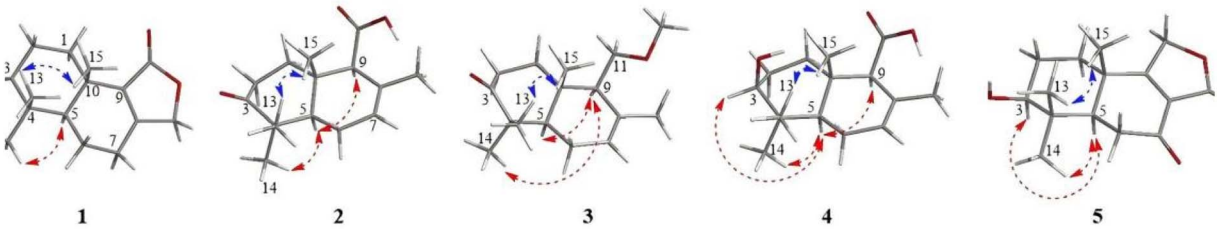

Fig. 3 Key ROESY correlations of compounds **1–5**.

replaced by a hydroxyl group. The structure of **4** was established with the aid of 1D and 2D NMR. From a biogenetic point of view, **4** seemed to be the precursor of **2**, suggesting that the relative configurations at C-5, C-9 and C-10 in **4** were the same as those in **2**. In the ROESY experiment, the cross-peaks between H-3/H-5, H-5/H-9 and CH_3-14/H-5 implied that H-3, H-5, H-9 and CH_3-14 were all α-oriented. In addition, the ROE correlations of CH_3-13 with CH_3-15 indicated that CH_3-13/15 were β-oriented (Fig. 3). Accordingly, the 3*S*, 5*R*, 9*S* and 10*S* absolute configuration was established from the similarity between the calculated ECD curves and the experimental ECD data (Fig. 4). Therefore, the structure of compound **4** was established as 3β-hydroxyl-drimenoic acid and named sinenseine D.

Compound **5** was isolated as a light-yellow oil, and it possessed a molecular formula of $C_{15}H_{20}O_4$, as deduced from the HRESIMS signal at *m*/*z* 263.1289 $[M - H]^-$ (calcd for $C_{15}H_{19}O_4$, 263.1283). The ^{1}H NMR spectrum of **5** (Table 1) showed an oxygenated methylene at δ_H 4.88 (2H, s), an oxygenated methine at δ_H 3.10 (1H, dd, J = 13.2, 6.6 Hz), and three single methyl groups at δ_H 1.19 (3H, s), 0.93 (3H, s) and 0.80 (3H, s). The ^{13}C NMR and HSQC spectra of **5** revealed 15 resonances, including a ketone carbonyl carbon at δ_C 195.9, an ester carbonyl carbon at δ_C 173.5, two olefinic carbons at δ_C 149.8 and 149.7, an oxygenated methylene carbon at δ_C 67.4, an oxygenated methine carbon at δ_C 75.8, and three methyl carbons at δ_C 27.5, 17.6 and 15.3. The characteristic carbon signal at δ_C 195.9 led us to consider it similar to compound **9**, and their 1D NMR data were found to be very similar. The notable difference between **5** and **9** was the presence of oxygenated methine moiety (δ_H 3.10, δ_C 75.8) in **5**. In addition, the position of the ester carbonyl group in **5** was also different, which caused the chemical shift of C-9 from δ_C 152.5 in **9** to 149.7 in **5**. This change was also confirmed by the key HMBC correlations of δ_H 4.88 (H-11) with δ_C 149.8 (C-8), 149.7 (C-9), 35.7 (C-10) and 17.6 (C-15) (Fig. 2). The relative configuration of **5** was determined on the basis of the NOESY spectrum. The correlations of CH_3-13/CH_3-15 indicated their β-orientation. Cross-peaks between H-3/H-5 and CH3-14/H-5 revealed that H-3, H-5 and CH_3-14 were α-oriented (Fig. 3). In addition, the constant coupling of H-3 (J = 13.2, 6.6 Hz) also supported that H-3 was α-oriented. The calculated ECD curve coincided well with the experimental ECD spectrum, and a 3*S*, 5*R*, 10*S* absolute configuration was established for **5** (Fig. 4). Therefore, the structure of compound **5** was assigned as shown in the figure and named sinenseine E.

Compound **6** was isolated as an amorphous yellow solid with an identical molecular formula of $C_{15}H_{24}O_3$ based on its HRESIMS data, indicating a deprotonated ion at *m*/*z* 251.1642 $[M - H]^-$ (calcd for $C_{15}H_{23}O_3$, 251.1647). The molecular weight of **6** was the same as that of **4** and their 1D NMR data were highly similar, except for the presence of oxygenated methylene [δ_H 3.15 (1H, d, J = 10.8 Hz), 2.85 (1H, d, J = 10.8 Hz); δ_C 70.2] in **6** and the absence of oxygenated methine [δ_H 3.24 (1H, m); δ_C 74.1] and methyl [δ_H 0.89 (1H, m); δ_C 28.9] in **4**. A detailed examination of the 1D NMR data showed that a hydroxyl group was linked with the methyl group, which was also supported by

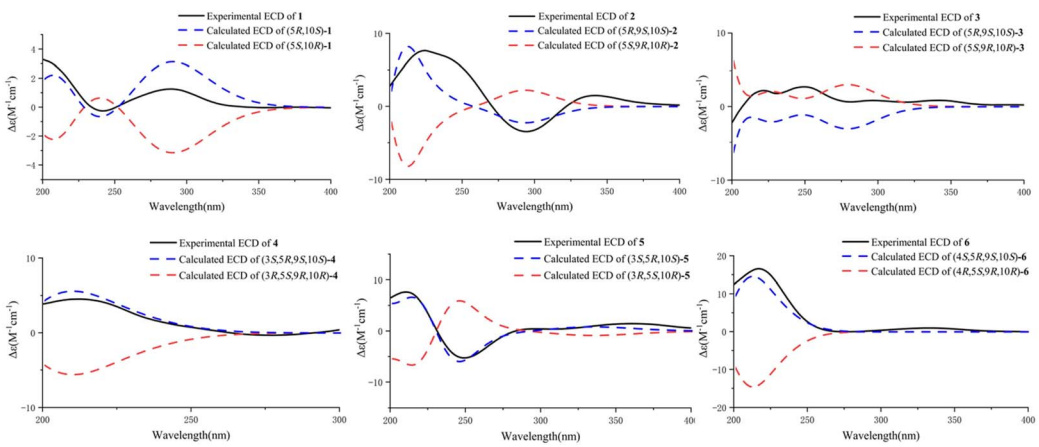

Fig. 4 Comparison of the calculated and experimental ECD spectra of compounds **1–6**.

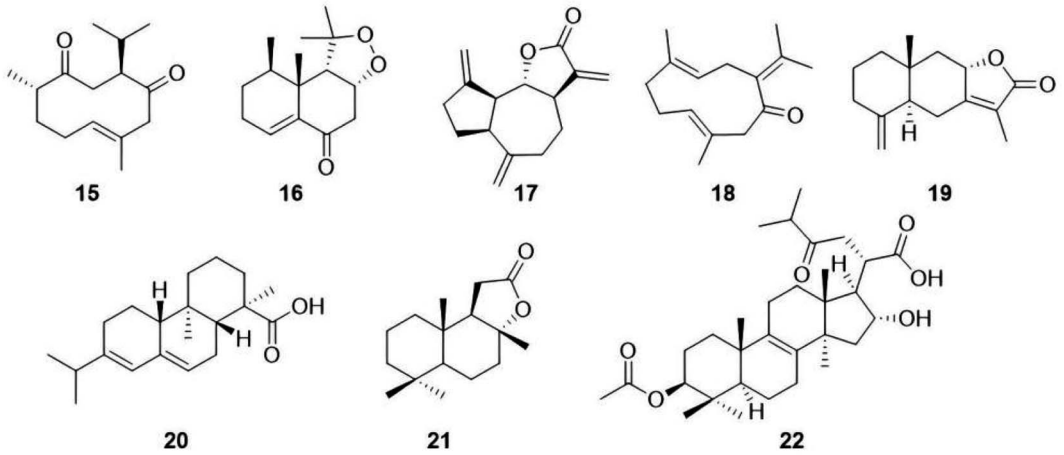

Fig. 5 Structures of the terpenoids identified by UPLC-MS/MS (**15–22**).

the key HMBC correlations of δ_H 3.15/2.85 (H-13) with δ_C 35.7 (C-3), 37.6 (C-4), and 18.3 (C-14) (Fig. 2). The planar structure of **6** was deduced from the 1D and 2D NMR data, including the key HMBC correlations of δ_H 3.15/2.85 (H-13) with δ_C 35.7 (C-3), 37.6 (C-4), and 18.3 (C-14) (Fig. 2). From a biogenetic point of view, the relative configuration at H-9 and CH_3-13/14/15 in **6** were the same as those of **1–5**. The calculated ECD data of 6 matched well with the experimental ECD curve, suggesting the absolute configuration of 6 to be 4*S*, 5*R*, 9*S* and 10*S* (Fig. 4). Hence, compound **6** was determined as 13-hydroxyl-drimenoic acid and named sinenseine F.

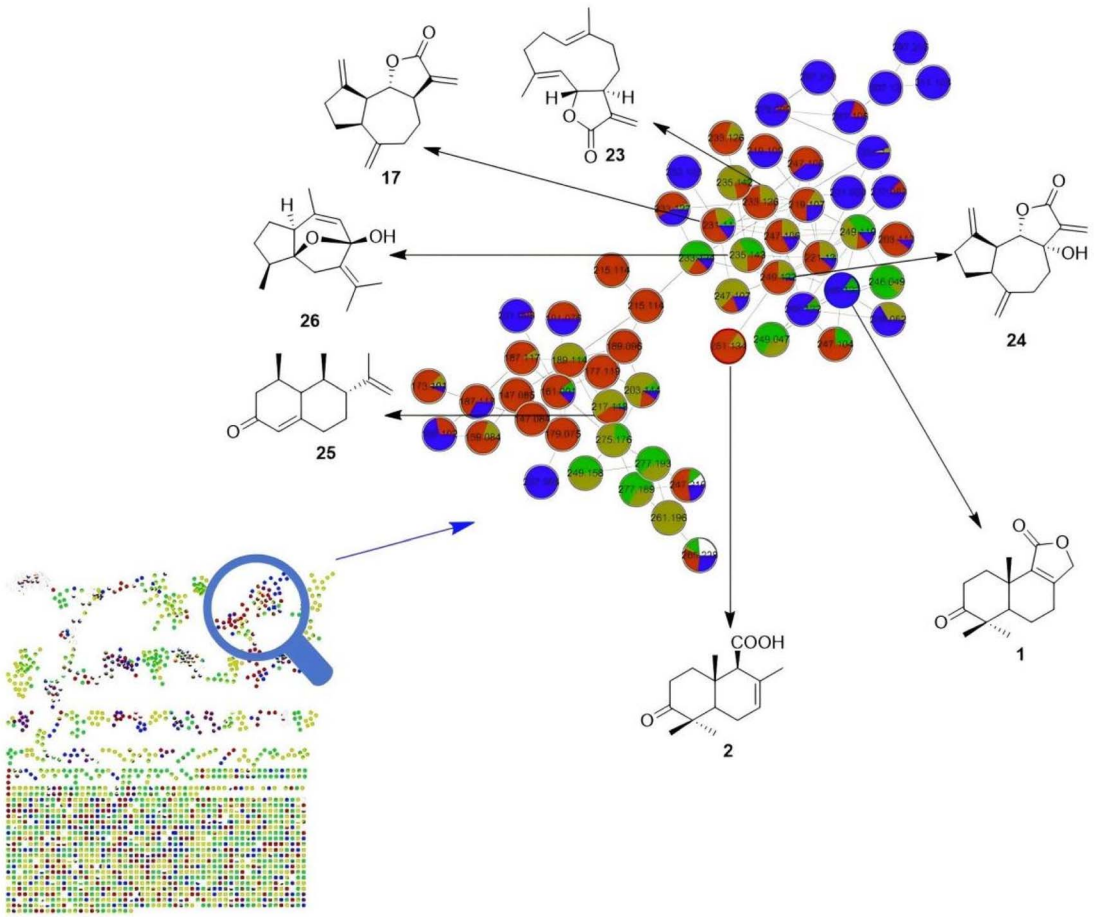

Fig. 6 Molecular network built using HPLC-MS/MS analyses of fractions from the *L. sinense* extract and the five identified sesquiterpenes (**17**,**23–26**).

Moreover, eight known compounds were also obtained from the whole plant of *L. sinense* and identified as 3β-hydroxy-drimenol (**7**),[11] 3-keto-drimenol (**8**),[11] 7-ketoisodrimenin (**9**),[10] inotolactones E (**10**),[12] oleanolic acid (**11**),[13] ursolic acid (**12**),[14] 19α-hydroxyl ursolic acid (**13**),[13] corsolic acid (**14**)[15] (Fig. 1) by comparing their NMR data with those reported in the literature.

UPLC-MS/MS and GNPS for the identification of terpenoids in *L. sinense*

At present, UPLC-MS/MS is widely used to analyse and identify the chemical constituents in medicinal plants. As shown in Fig. 5, in this study, we identified five sesquiterpenes, namely curdione (**15**),[16] nardosinone (**16**),[17] dehydrocostus lactone (**17**),[18] germacrone (**18**)[16] and atractylenolide II (**19**),[19] two diterpenes named abietic acid (**20**)[20] and sclareolide (**21**),[21] and a triterpenoid named pachymic acid (**22**)[22] from the *L. sinense* extract using the UPLC-MS/MS method in combination with database comparison. In addition, we tried identifying more sesquiterpenoid analogues from *L. sinense* using the GNPS method, and the secondary mass spectrometry fragment ions of compounds **1** and **2** were used as references. However, drimane-type sesquiterpenoids were not found, but five other-type sesquiterpenoids were identified, including dehydrocostus lactone (**17**),[18] costunolide (**23**),[23] 7α-hydroxy-3-desoxyzaluzanin C (**24**),[24] (+)-nootkatone (**25**)[25] and curcumenol (**26**)[26] (Fig. 6). Although these identified terpenoids must be verified using standard substances, it can be deduced that *L. sinense* extracts are rich in terpenoids, including sesquiterpenoids, diterpenes and triterpenoids, based on these identified and isolated compounds. Thus, the search for the synthesis of more terpenoids from *L. sinense* needs to be further intensified.

Antiproliferative and anti-inflammatory activities of compounds 1–14

In our previous study, we found that the EtOAc-soluble extract of *L. sinense* exhibited significant anti-inflammatory activity, with an inhibition rate of 90.7% ± 3.2% at 50 μg mL^{-1} against LPS-induced Nitric Oxide (NO) production in RAW264.7 cells.[27] Previous works have also revealed that drimane-type sesquiterpenoids possess different levels of antiproliferative effects on cancer cells, such as HL-60, MCF-7, A549, H1299, HepG2 and A2780.[28] Thus, all isolates were evaluated for antiproliferative and anti-inflammatory activities *in vitro* (Table 3). The results revealed that compounds **2–4**, **6**, **13** and **14** had moderate antiproliferative effects on A549, H1299, HepG2 and A2780 cells, with IC_{50} values ranging from 35.2 ± 2.0 to 90.5 ± 3.1 μM. Disappointingly, no compound showed a significant anti-tumor effect. However, this is consistent with the results reported in the review, indicating that drimane-type sesquiterpenoids may not have strong cytotoxicity to induce tumor cell apoptosis.[28] To assess the structure–activity relationship of the isolates, a comparison of the cytotoxic effects of **2** and **4** indicated that the hydroxyl group associated with C-3 might play an important role in the antiproliferative effect. As for anti-inflammatory activity, compounds **1**, **2**, **5**, **7**, **8** and **14** showed different levels of activity, with IC_{50} values ranging from 8.3 ± 1.2 to 48.4 ± 2.3 μM against NO production. Among these compounds, **1** displayed the highest anti-inflammatory activity with an IC_{50} value of 8.3 ± 1.2 μM. A comparison of the anti-inflammatory activities of **3**, **7** and **8** indicated that the ketone group associated with C-3 was more potent than the methoxy group. In addition, **2** (IC_{50} = 19.4 ± 0.8 μM) displayed higher activity than **4** (IC_{50} > 50 μM). This also indicates that the ketone group located at C-3 might have a positive effect on the anti-inflammatory activity.

According to the literature, most drimane-type sesquiterpenoids are isolated from fungi, such as *Aspergillus parasiticus*, *Penicillium roqueforti* and marine fungus *Paraconiothyrium sporulosum*, in which they function as secondary metabolites.[29–31] However, not many drimane-type sesquiterpenoids have been isolated from plants. This differentiation caught our interest and a careful literature survey was conducted in order to find some chemotaxonomic markers and clarify the difference between drimane-type sesquiterpenoids isolated from plants and fungi. For this purpose, 27 published articles describing drimane-type sesquiterpenoids from plants were summarized, and no significant differences were found. Drimane-type sesquiterpenoids belong to a unique sesquiterpenoid family and possess various bioactivities, such as anti-tumor, anti-inflammatory, neuroprotective and antimicrobial activities. Until now, this type of sesquiterpenes has not been studied in depth. This study provides a new approach to identify more effective drimane-type sesquiterpenoids. Moreover, it is essential to explore other salt-tolerant plants for drimane-type sesquiterpenes.

Experimental

General procedures

Optical rotation was measured with an AUTOPOL IV automatic polarimeter (Rudolph Research Analytical, USA). The UV spectra were measured on a Shimadzu UV-2401A spectrophotometer (Shimadzu, Tokyo, Japan). The IR spectra were recorded using an FTIR-8400S spectrometer with KBr discs (Shimadzu, Tokyo, Japan). The ECD spectra were obtained on an ECD spectrometer (Biologic MOS 450, France). The nuclear magnetic resonance (NMR) spectra were obtained using a Bruker AV-600 spectrometer (Bruker, Karlsruhe, Germany) with TMS as the internal standard. The mass spectra were obtained on a Bruker micro-TOF-Q mass spectrometer (Bruker, Karlsruhe, Germany). Column chromatography was performed using silica gel (200–300 μm particle size, Qingdao Marine Chemical Co., Ltd., Qingdao, China) and RP-18 (150–63 μm particle size, Merck, Darmstadt, Germany). TLC was performed with precoated silica gel GF_{254} glass plates (Qingdao Marine Chemical Co., Ltd). HPLC was carried out using a Shimadzu System LC-20AD pump equipped with a UV detector model SPD-20Avp (Shimadzu, Tokyo, Japan) and a YMC Pack ODS-A column (5 μm, 20 × 250 mm).

Plant material

The whole plant of *L. sinense* was collected in June 2022 from Dongying, Shandong province, China (east longitude: 118°

35′53″; north latitude: 37°18′10″) and authenticated by Associate Prof. Miao Wang (School of Traditional Chinese Medicine, Shenyang Pharmaceutical University). A specimen of this plant (No. LS-20220620) was deposited at the Medical Research Center, Binzhou Medical University Hospital, Binzhou, China.

Extraction and isolation

The dried whole plant of *L. sinense* (50.0 kg) were extracted three times with 70% EtOH, and 4.96 kg of crude extract was obtained. Then, this extract was suspended in H_2O and partitioned using petroleum ether (PE), CH_2Cl_2, EtOAc and *n*-BuOH, successively. The EtOAc fraction (160.2 g) was subjected to silica gel column chromatography (CC) using a gradient of CH_2Cl_2–MeOH (from 100 : 1 to 0 : 1) to give 21 fractions (Fr.1–Fr.21). Fr.7 (4.9 g) was applied to a silica gel CC using a gradient of PE-EtOAc (from 1 : 0 to 0 : 1) as the eluent, which yielded 12 fractions (Fr.7.1–Fr.7.12). Furthermore, Fr.7.1 (835.5 mg) was further purified by HPLC and eluted with an isocratic solvent system of 50% MeOH in H_2O at a flow rate of 1.5 mL min^{-1} over 70 min, and 10 fractions were collected (Fr.7.1.1–Fr.7.1.10). Fr.7.1.5 (183.1 mg) was purified by HPLC and eluted with an isocratic solvent system of 35% MeOH in H_2O at a flow rate of 1.5 mL min^{-1} over 60 min to isolate compounds **6** (20.8 mg, t_R = 32.5 min), **4** (6.2 mg, t_R = 39.4 min), **2** (5.9 mg, t_R = 45.0 min) and **1** (15.2 mg, t_R = 54.3 min). Fr.7.1.7 (154.3 mg) was separated by HPLC, using an isocratic solvent system of 45% MeOH in H_2O at a flow rate of 1.5 mL min^{-1} over 70 min to isolate compounds **7** (3.2 mg, t_R = 27.2 min), **10** (4.6 mg, t_R = 32.6 min), **3** (6.4 mg, t_R = 37.8 min), **5** (10.5 mg, t_R = 42.1 min), **8** (8.4 mg, t_R = 48.6 min) and **9** (2.8 mg, t_R = 53.7 min). Fr.7.1.9 (108.4 mg) was separated by HPLC using an isocratic solvent system of 80% ACN in H_2O at a flow rate of 1.5 mL min^{-1} over 60 min to isolate compounds **14** (5.0 mg, t_R = 23.6 min), **11** (25.1 mg, t_R = 30.7 min), **13** (28.4 mg, t_R = 35.0 min) and **12** (34.1 mg, t_R = 38.5 min).

Sinenseine A (**1**): amorphous light yellow solid; [α] −29.5 (*c* 0.1, MeOH); UV (MeOH) λ_{max} (log ε): 207 (2.32), 220 (2.03) nm; IR (KBr disc) ν_{max} 1765, 1628, 1448, 1404 cm^{-1}; ^{1}H NMR (600 MHz, DMSO-d_6) and ^{13}C NMR (150 MHz, DMSO-d_6) data, see Tables 1 and 2; HRESIMS: *m*/*z* 247.1340 $[M - H]^-$ (calcd for $C_{15}H_{19}O_3$, 247.1334).

Sinenseine B (**2**): amorphous yellow solid; [α] −37.8 (*c* 0.1, MeOH); UV (MeOH) λ_{max} (log ε): 206 (2.02) nm; IR (KBr disc) ν_{max} 3408, 2874, 1762, 1718, 1664, 1457 cm^{-1}; ^{1}H NMR (600 MHz, DMSO-d_6) and ^{13}C NMR (150 MHz, DMSO-d_6) data, see Tables 1 and 2; HRESIMS: *m*/*z* 249.1496 $[M - H]^-$ (calcd for $C_{15}H_{21}O_3$, 249.1491).

Sinenseine C (**3**): amorphous light yellow solid; [α] −43.4 (*c* 0.1, MeOH); UV (MeOH) λ_{max} (log ε): 210 (2.64) nm; IR (KBr disc) ν_{max} 1774, 1632, 1431 cm^{-1}; ^{1}H NMR (600 MHz, DMSO-d_6) and ^{13}C NMR (150 MHz, DMSO-d_6) data, see Tables 1 and 2; HRESIMS: *m*/*z* 249.1849 $[M - H]^-$ (calcd for $C_{16}H_{25}O_2$, 249.1855).

Sinenseine D (**4**): amorphous yellow solid; [α] −29.2 (*c* 0.1, MeOH); UV (MeOH) λ_{max} (log ε): 204 (2.83) nm; IR (KBr disc) ν_{max} 3423, 2935, 1740, 1632, 1407 cm^{-1}; ^{1}H NMR (600 MHz, DMSO-d_6) and ^{13}C NMR (150 MHz, DMSO-d_6) data, see Tables 1 and 2; HRESIMS: *m*/*z* 251.1652 $[M - H]^-$ (calcd for $C_{15}H_{23}O_3$, 251.1647).

Sinenseine E (**5**): light yellow oil; [α] +53.6 (*c* 0.1, MeOH); UV (MeOH) λ_{max} (log ε): 203 (3.23) nm; IR (KBr disc) ν_{max} 3563, 3472, 1747, 1672, 1436 cm^{-1}; ^{1}H NMR (600 MHz, DMSO-d_6) and ^{13}C NMR (150 MHz, DMSO-d_6) data, see Tables 1 and 2; HRESIMS: *m*/*z* 263.1289 $[M - H]^-$ (calcd for $C_{15}H_{19}O_4$, 263.1283).

Sinenseine F (**6**): amorphous yellow solid; [α] −42.1 (*c* 0.1, MeOH); UV (MeOH) λ_{max} (log ε): 203 (2.45) nm; IR (KBr disc) ν_{max} 3436, 2963, 2867, 1778, 1458 cm^{-1}; ^{1}H NMR (600 MHz, DMSO-d_6) and ^{13}C NMR (150 MHz, DMSO-d_6) data, see Tables 1 and 2; HRESIMS: *m*/*z* 251.1642 $[M - H]^-$ (calcd for $C_{15}H_{23}O_3$, 251.1647).

Table 3 Antiproliferative and anti-inflammatory activities (inhibition on NO production) of compounds **1–14** (IC_{50} μM)

	Cytotoxicity[b]				
Compounds	A549	H1299	HepG2	A2780	Anti-inflammatory activity[b]
1	>100	>100	>100	>100	8.3 ± 1.2
2	82.9 ± 2.4	75.4 ± 2.9	65.2 ± 2.3	57.9 ± 3.1	19.4 ± 0.8
3	>100	>100	>100	89.1 ± 2.8	>50
4	62.8 ± 1.9	71.3 ± 2.8	50.1 ± 2.2	35.2 ± 2.0	>50
5	>100	>100	>100	>100	13.4 ± 1.0
6	78.0 ± 1.7	78.2 ± 2.6	80.8 ± 2.5	>100	>50
7	>100	>100	>100	>100	38.5 ± 2.1
8	>100	>100	>100	>100	23.0 ± 1.7
9	>100	>100	>100	>100	>50
10	>100	>100	89.6 ± 2.7	>100	>50
11	>100	>100	>100	>100	>50
12	>100	>100	>100	>100	>50
13	83.7 ± 2.9	80.2 ± 2.3	>100	65.0 ± 2.7	>50
14	90.5 ± 3.1	>100	88.5 ± 2.6	>100	48.4 ± 2.3
Doxorubicin[a]	1.02 ± 0.7	1.24 ± 0.9	0.86 ± 0.5	0.21 ± 0.1	—
Dexamethasone[a]	—	—	—		0.58 ± 0.2

[a] Positive control. [b] Data are represented as mean ± SD (n = 3).

Qualitative study of terpenoids in *L. sinense* by UPLC-MS/MS and molecular network analysis

UPLC-Q Exactive Orbitrap-MS/MS was used for the qualitative analysis of the chemical constituents of *L. sinense*, and the 70% EtOH extract of the whole plant of *L. sinense* was taken for analysis. The ACQUITY UPLC HSS T3 column (2.1 × 100 mm, 1.8 μm) was used for gradient elution with acetonitrile solution (B) 0.1% aqueous formic acid solution (A) as the mobile phase. The elution parameters were as follows: column temperature, 35 °C; flow rate, 0.3 mL min; injection volume, 10 μL; the detection mode was Full MS-ddMS^2; the positive ion and negative ion modes were scanned separately. The scanning range was *m*/*z* 100–1200; the MS resolution was set to 70 000; the MS^1 rate was set to 70 000, and the MS^2 rate was set to 17 500; the ion source voltage was 3.2 kV; the capillary ion transfer tube temperature was 320 °C; the auxiliary gas heating temperature was 350 °C; and the sheath gas flow rate was 40 L min^{-1}. The auxiliary gas velocity was 15 L min^{-1}, the AGC Target was set to 1 × 10^6, the TopN was set to 5, and the collision energy to trigger the MS^2 scan was set to 30, 40, and 50 using the stepped fragmentation voltage NCE. Compound Discover 3.2 software was used to extract the characteristic peaks from raw mass spectrometry data, and the mass deviations for characteristic peak element matching, molecular formula prediction and isotope distribution matching were all set to less than 5 ppm. The characteristic peaks were identified using the mzcloud online database and a local self-built mzVault Traditional Chinese Medicine natural products database. The screening criterion for positive results was mass deviation <5 ppm. When the results were consistent with the isotope distribution and mzVault best match database, the score was >70. In addition, the MS/MS data files were converted to the .mzXML format using the MSConvert software. The molecular network was constructed using the GNPS (**http://gnps.ucsd.edu**) data analysis workflow and the spectral clustering algorithm. The spectral networks were imported into Cytoscape 3.8.2 for visualization.

ECD computations

Conformational searches and the establishment of low-energy conformers for compounds **1–6** were carried out using Spartan 1.1.4 software. Next, all selected conformations with a suitable Boltzmann distribution of more than 1% were reoptimized at the B3LYP/6-31G (d) level by DFT calculations in the GAUSSIAN 09 program. Subsequently, the ECD curves of the reoptimized conformers were calculated using the time-dependent density functional theory (TDDFT) method at the B3LYP/6-31G (d, p) level in MeOH. All simulated spectra of these conformations were averaged with the lowest Gibbs free energy according to the Boltzmann distribution theory using the SpecDis 1.71 software.[32]

Anti-inflammatory assays

The RAW 264.7 macrophage cell line was purchased from Wuhan Boster Biological Technology., LTD. The *in vitro* anti-inflammatory activity was evaluated by measuring the NO production inhibitory rates of the compounds in LPS-induced RAW264.7 cells.[33] Briefly, the RAW264.7 cells were plated in a 96-well plate at a density of 5 × 10^4 cells per well, and the CKK8 assay was used to establish that the compounds were not cytotoxic within a certain concentration range. Dexamethasone was used as the positive control. A Griess kit was used to measure the effect of the compounds at different concentrations against NO secretion induced by LPS in RAW 264.7 cells. The absorbance was measured at 540 nm by a Varioskan flash instrument. NO production was calculated using the $NaNO_2$ standard curve, and minocycline was used as the positive control.

Anti-tumor assays

The CCK8 assay was used to evaluate the cytotoxicity of isolated compounds **1–14** according to the published method.[13] A549, HepG2, H1299 and A2780 cancer cells were purchased from Wuhan Boster Biological Technology., LTD. Briefly, the cells were harvested using trypsin, seeded in 96-well plates at 5000 cells per well and then incubated for 12 h. The test samples dissolved in DMSO were added to each well, and the cells were incubated for another 48 hours. Control wells were treated with 1% aqueous DMSO, and doxorubicin was used as the positive control. After 48 h of incubation, 10 μL of CCK8 was added to each well and incubated for 3–4 h at 37 °C with 5% CO_2. The absorbance of each well was measured at 450 nm using a microplate reader (Thermo Scientific Multiskan MK3, Shanghai, China).

Conclusions

In summary, lots of saline-tolerant medicinal plants in YRD possess high values and need to be deeply studied. In the present work, we isolated fourteen terpenoids including ten drimane-type sesquiterpenoids and four triterpenoids from the whole plant of *L. sinense* for the first time. Based on the cytotoxicity results of these isolates and the bioactivity of 164 reported drimane-type sesquiterpenoids, we found that most of the isolated drimane-type sesquiterpenes may not have a strong ability to directly kill tumor cells. In addition, some isolates showed potential anti-inflammatory activity, and **1** displayed the highest anti-inflammatory activity with an IC_{50} value of 8.3 ± 1.2 μM against NO production. Furthermore, twelve terpenoids, including nine sesquiterpenoids, two diterpenes and a triterpenoid, were identified by UPLC-MS/MS and GNPS methods. Our work demonstrates that *L. sinense* extracts are rich in terpenoids, and the study of the bioactivity of drimane-type sesquiterpenes should be further expanded beyond anti-tumor activity.

Data availability

The data supporting the findings of this study are available within the article and its ESI.†

Author contributions

S. Z. Q. conceived, designed, and supervised the research project, as well as revised the manuscript; K. K. G. and S. M. supervised the anti-inflammatory and anti-tumor activity assays and revised the manuscript; X. Y. Meng, B. J. Cui and T. T. Liu performed the experiments and prepared the manuscript, L. J. Yang analyzed the NMR data; G. W. Cai provided comments and suggestions on the preparation of the manuscript and performing the experiments.

Conflicts of interest

The authors declare no conflict of interest.

Acknowledgements

This work was financially supported from the Natural Science Foundation of Shandong Province (ZR2023QH153), Research Foundation of Binzhou Medical University (BY2021KYQD30) and Binzhou Medical University "Clinical + X" project (BY2021LCX23), Shandong Provincial Medical and Health Science and Technology Development Plan (202313050516).

References

1 S. T. Fang, X. Liu, N. N. Kong, S. J. Liu and C. H. Xia, Two new withanolides from the halophyte *Datura stramonium* L, *Nat. Prod. Res.*, 2013, **27**, 1965–1970.
2 Q. Liu, H. Y. Liu, J. C. Dou, F. Q. Zhou, H. Zhang, X. Q. Hu, X. Y. Zhang and Y. Q. Zhang, Investigation of aquatic salt-tolerant medicinal plant resources in the Yellow River Delta and development and utilization of characteristic medicinal plants, *Mod. Chin. Med.*, 2023, **25**, 244–251.
3 H. L. Zhao, S. Y. Wang, P. T. F. Williamson, R. M. Ewing, X. H. Tang, J. L. Wang and Y. H. Wang, Integrated network pharmacology and cellular assay reveal the biological mechanisms of *Limonium sinense* (Girard) Kuntze against breast cancer, *BMC, Complement. Med.*, 2023, **23**, 408.
4 Editorial Committee of Chinese Herbal and The State Administration of Traditional Chinese Medicine, *Chinese Herbal*, Shanghai Science and Technology Publishers, Shanghai, 1999, vol XVI, p. 130.
5 H. L. Zhao, S. Y. Wang, Y. L. Zhou, A. Ertay, P. T. F. Williamson, R. M. Ewing, X. H. Tang, J. L. Wang and Y. H. Wang, Integrated analysis reveals efects of bioactive ingredients from *Limonium sinense* (Girard) Kuntze on hypoxia-inducible factor (HIF) activation, *Front. Plant Sci.*, 2022, **13**, 994036.
6 W. C. Hsu, S. P. Chang, L. C. Lin, C. L. Li, C. D. Richardson, C. C. Lin and L. T. Lin, *Limonium sinense* and gallic acid suppress hepatitis C virus infection by blocking early viral entry, *Antivir. Res.*, 2015, **118**, 139–147.
7 X. H. Tang, J. Gao, J. Chen, L. Z. Xu, Y. H. Tang, X. N. Zhao and L. Michael, Mitochondrial modulation is involved in the hepatoprotection of *Limonium sinense* extract against liver damage in mice, *J. Ethnopharmacol.*, 2008, **120**, 427–431.
8 X. H. Tang, L. F. Yan, J. Gao, X. L. Yang, X. X. Xu, H. Y. Ge and H. D. Yang, Antitumor and immunomodulatory activity of polysaccharides from the root of *Limonium sinense* Kuntze, *Int. J. Biol. Macromol.*, 2012, **51**, 1134–1139.
9 L. C. Lin and C. J. Chou, Flavonoids and phenolics from *Limonium sinense*, *Planta Med.*, 2000, **66**, 382–383.
10 N. Allouche, C. Apel, M. T. Martin, V. Dumontet, F. Guéritte and M. Litaudon, Cytotoxic sesquiterpenoids from winteraceae of Caledonian rainforest, *Phytochemistry*, 2009, **70**, 546–553.
11 D. Xu, Y. Sheng, Z. Y. Zhou, R. Liu, Y. Leng and J. K. Liu, Sesquiterpenes from cultures of the basidiomycete Clitocybe conglobata and their 11β-hydroxysteroid dehydrogenase inhibitory activity, *Chem. Pharm. Bull.*, 2009, **57**, 433–435.
12 C. X. Zou, X. B. Wang, T. M. Lv, Z. L. Hou, B. Lin, X. X. Huang and S. J. Song, Flavan derivative enantiomers and drimane sesquiterpene lactones from the *Inonotus obliquus* with neuroprotective effects, *Bioorg. Chem.*, 2020, **96**, 103588.
13 S. Z. Qi, T. Liu, M. Wang, X. X. Zhang, Y. R. Yang, W. H. Jing, L. P. Long, K. R. Song, Y. Jin and H. Y. Gao, New phenylpropanoid-conjugated pentacyclic triterpenoids from the whole plants of *Leptopus lolonum* with their antiproliferative activities on cancer cells, *Bioorg. Chem.*, 2021, **107**, 104628.
14 S. H. Ghoran, O. Firuzi, M. Asadollahi, H. Stuppner, M. Alilou and A. R. Jassb, Dammarane-type triterpenoid saponins from *Salvia russellii* Benth, *Phytochemistry*, 2021, **184**, 112653.
15 S. Khan, M. Nisar, R. Khan, W. Ahmad and F. Nasir, Evaluation of chemical constituents and antinociceptive properties of *Myricaria elegans* Royle, *Chem. Biodivers.*, 2010, **7**, 2897–2900.
16 L. Li, Q. Xie, G. Bian, B. Y. Zhang, M. F. Wang, Y. P. Wang, Z. J. Chen and Y. S. Li, Anti-H1N1 viral activity of three main active ingredients from zedoary oil, *Fitoterapia*, 2020, **142**, 104489.
17 J. W. Wen, L. Q. Liu, J. J. Li and Y. He, A review of nardosinone for pharmacological activities, *Eur. J. Pharmacol.*, 2021, **908**, 174343.
18 K. Cao, W. Qian, Y. Xu, Z. Zhou, Q. Zhang and X. F. Zhang, A new sesquiterpenoid from *Saussurea lappa* roots, *Nat. Prod. Res.*, 2016, **30**, 2160–2163.
19 N. Zhang, C. Liu, T. M. Sun, X. K. Ran, T. G. Kang and D. Q. Dou, Two new compounds from *Atractylodes macrocephala* with neuroprotective activity, *J. Asian Nat. Prod. Res.*, 2017, **19**, 35–41.
20 N. Y. Yang, L. Liu, W. W. Tao, J. A. Duan and L. J. Tian, Diterpenoids from *Pinus massoniana* resin and their cytotoxicity against A431 and A549 cells, *Phytochemistry*, 2010, **71**, 1528–1533.
21 Q. Chen, K. Tang and Y. Guo, Discovery of sclareol and sclareolide as filovirus entry inhibitors, *J. Asian Nat. Prod. Res.*, 2020, **22**, 464–473.
22 K. H. Lai, M. C. Lu, Y. C. Du, M. El-Shazly, T. Y. Wu, Y. M. Hsu, A. Henz, J. C. Yang, A. Backlund, F. R. Chang

and Y. C. Wu, Cytotoxic lanostanoids from *Poria cocos*, *J. Nat. Prod.*, 2016, **79**, 2805–2813.

23 C. Lu, X. Y. Li, W. X. Du, X. Zhang, Y. P. Li, C. Y. Hu, Z. W. Mao, Y. Zhang and R. R. Wang, Exploration of costunolide derivatives as potential anti-inflammatory agents for topical treatment of atopic dermatitis by inhibiting MAPK/NF-κB pathways, *Bioorg. Chem.*, 2024, **143**, 107054.

24 D. H. De Luengo, M. Miski, D. A. Gage and T. J. Mabry, 7α-Hydroxy-sesquiterpene lactones from *Decachaeta ovatifolia*, *Phytochemistry*, 1986, **25**, 1917–1922.

25 Y. Guo, E. H. Hou, N. N. Ma, Z. Y. Liu, J. P. Fan and R. G. Yang, Discovery, biological evaluation and docking studies of novel N-acyl-2-aminothiazoles fused (+)-nootkatone from *Citrus paradisi* Macf. as potential α-glucosidase inhibitors, *Bioorg. Chem.*, 2020, **104**, 104294.

26 C. X. Zhou, L. S. Zhang, F. F. Chen, H. S. Wu, J. X. Mo and L. S. Gan, Terpenoids from *Curcuma wenyujin* increased glucose consumption on HepG2 cells, *Fitoterapia*, 2017, **121**, 141–145.

27 S. Z. Qi, G. F. Qin, S. Miao, W. Y. Lv, S. Q. Ren, K. K. Gong, Y. Q. Zhang and J. Du, Chemical constituents from the whole plants of *Limonium sinense* and their *in vitro* anti-inflammatory activity, *Chem. Biodivers.*, 2024, e202401514.

28 W. Y. Du, Q. Yang, H. M. Xu and L. B. Dong, Drimane-type sesquiterpenoids from fungi, *Chin. J. Nat. Med.*, 2022, **20**, 737–748.

29 G. Z. Dai, J. P. Sun, X. P. Peng, Q. Y. Shen, C. Z. Wu, Z. H. Sun, H. Y. Sui, X. M. Ren, Y. M. Zhang, X. Y. Bian and R.-W. Astellolides, drimane-type sesquiterpenoids from an *Aspergillus parasiticus* Strain associated with an isopod, *J. Nat. Prod.*, 2023, **86**, 1746–1753.

30 H. Q. Li, R. G. Zhang, F. Cao, J. P. Wang, Z. X. Hu and Y. H. Zhang, Proversilins A-E, drimane-type sesquiterpenoids from the endophytic *Aspergillus versicolor*, *J. Nat. Prod.*, 2020, **83**, 2200–2206.

31 L. H. Zhang, G. Chen, Y. Sun, H. F. Wang, J. Bai, H. M. Hua and Y. H. Pei, Seven new drimane-type sesquiterpenoids from a marine-derived fungus *paraconiothyrium sporulosum* YK-03, *Molecules*, 2019, **24**, 1817.

32 M. Wang, S. Y. Yu, B. H. Zhang, K. R. Song, T. Liu and H. Y. Gao, Anti-inflammatory cassane-type diterpenoids from the seed kernels of *Caesalpinia sinensis*, *J. Nat. Prod.*, 2021, **84**, 2175–2188.

33 S. Z. Qi, Y. R. Yang, X. Y. Xian, X. Z. Li and H. Y. Gao, A new sesquiterpenoid glycoside from *Saussurea involucrata*, *Nat. Prod. Res.*, 2020, **34**, 943–949.